REPORT DOCUMENTATION PAGE

Form Approved OMB no. 0704-0188

1. AGENCY USE ONLY *(Leave blank)*

2. REPORT DATE
10 July 2001

3. REPORT TYPE AND DATES COVERED
Final Report: 15 November 1999 – 31 December 2000

4. TITLE AND SUBTITLE
Air-Sea Fluxes at High Winds

5. FUNDING NUMBERS
N00014-00-1-0149

6. AUTHOR(S)
Dr. Wade R. McGillis

7. PERFORMING ORGANIZATION NAME(S) AND ADDRESS(ES)
Applied Ocean Physics and Engineering Department
Woods Hole Oceanographic Institution
98 Water Street
Woods Hole, MA 02543-1053

8. PERFORMING ORGANIZATION REPORT NUMBER
13014900

9. SPONSORING/MONITORING AGENCY NAME(S) AND ADDRESS(ES)
Office of Naval Research

10. SPONSORING/MONITORING AGENCY REPORT NUMBER
N00014-00-1-0149

11. SUPPLEMENTARY NOTES

12a. DISTRIBUTION/AVAILABILITY STATEMENT
Approved for public release; distribution is unlimited

12b. DISTRIBUTION CODE

13. ABSTRACT *(Maximum 200 words)*

See attached report

14. SUBJECT TERMS
momentum and sensible heat fluxes, air-sea boundary layer, meteorology

15. NUMBER OF PAGES
16

16. PRICE CODE

17. SECURITY CLASSIFICATION OF REPORT	18. SECURITY CLASSIFICATION OF THIS PAGE	19. SECURITY CLASSIFICATION OF ABSTRACT	20. LIMITATION OF ABSTRACT
Unclassified	Unclassified	Unclassified	Unlimited

20010717 095

Air–Sea Fluxes at High Winds

Wade R. McGillis
Applied Ocean Physics and Engineering
Woods Hole Oceanographic Institution
Woods Hole, Massachusetts 02543
phone: (508) 289-3325 fax: (508) 457-2194 email: wmcgillis@whoi.edu
Award Number: N00014-00-1-0149
15 November 1999 – 31 December 2000
http://www.whoi.edu/science/AOPE/airsea/airsea.htm

LONG-TERM GOAL

The long-term goal was to improve our understanding of the detailed mechanism of momentum and energy flux from wind to surface waves, and to study turbulent energy and momentum transfer from surface waves to near-surface currents. Particularly in high winds, where the role of wind-wave and wave-current interactions in the formation of coherent structures is elusive. In high winds, autonomous direct flux measurements are necessary to explore the mechanisms of momentum and energy transfer throughout their respective boundary layers.

SCIENTIFIC OBJECTIVES

The primary scientific objective of this project was to maintain an autonomous flux system and data analysis of a sonic anemometer deployed at the United States Coast Guard (USCG) permanent tower at the mouth of Buzzards Bay, Massachusetts. Predominant winds during the summer, originating from the southwest, have almost unlimited fetch over the North Atlantic Ocean. Regular trips on the small WHOI coastal vessel Mytilus were performed to collect data stored on the tower and refurbish batteries. Momentum fluxes were calculated by three distinct methods: (1) direct covariance; (2) inertial-dissipation; and (3) bulk parameterization.

APPROACH

Determination of turbulent momentum and heat fluxes at the air-sea interface is an important component in the accurate characterization of the coupled atmosphere-ocean system. The interdependence between atmospheric motion and ocean dynamics is well established, and any coupled atmosphere-ocean model requires these fluxes as boundary conditions. As a general rule, at high winds momentum is transferred from atmosphere to ocean and water vapor is transferred in the opposite direction. However, energy and momentum are exchanged in a complicated manner involving a variety of factors such as wind speed, changing wind direction, wind growth and decay, stability, wave age and height, water depth, sea spray, fetch, and currents. Improved understanding of air-sea interaction processes will contribute to both oceanic and atmospheric models involving the marine boundary layer.

Much of the data related to turbulent fluxes has been gathered from ships because of the accessibility to the open ocean. However, ships are disadvantageous because of (1) substantial flow distortion, (2) sensor motion, (3) relatively short deployments, (4) exclusion of the high wind speed regimes and (5) possible heat island effects. Autonomous measurements from a fixed stable platform could reduce or completely eliminate each of these problems.

For this investigation, a sonic anemometer-thermometer was deployed starting in December 1999 until April 2001 at the Buzzards Bay Tower off Massachusetts. One advantage of this tower is that it is a National Data Buoy Center (NDBC) CMAN station where mean atmospheric and oceanic information is regularly collected. This allowed for correlation with the data collected for this investigation. Predominant winds during the summer, originating from the southwest, have an almost unlimited fetch (wave development) over the North Atlantic Ocean.

Momentum and heat fluxes were calculated by three distinct methods:

- direct covariance
- inertial-dissipation
- bulk parameterization

A fourth alternative, the profile method, has not been widely used over the ocean. Direct covariance is considered to be the standard method since direct measurements provide fluxes [Large and Pond, 1981], whereas the other two methods depend on models. Using turbulent statistics, inertial-dissipation is more direct than bulk methods. Comparisons among these methods were performed.

The primary impetus behind this project was determination of the feasibility of measurements from the Buzzards Bay Tower.

Theoretical Background

Velocity components and temperature in turbulent flow follow the general decomposition $X(t) = \overline{X} + x'(t)$ where X is the measured velocity or temperature, $\overline{X}$ is the local mean flow and x' represents the random turbulent fluctuations with zero mean. Within the postulated constant stress layer, fluxes are carried by these turbulent fluctuations. Methods used to analyze fluxes at the tower are provided in the following three subsections.

Bulk Parameterization.

The first method utilized the TOGA COARE bulk parameterization [Fairall et al., 1996] based largely on the model proposed by Liu et al. [1979] using bulk transfer coefficients. This bulk flux algorithm has inputs of sea temperature, air temperature, relative humidity, horizontal wind speed, atmospheric pressure and instrument heights, returning the fluxes

of sensible heat, latent heat and momentum along with the associated friction velocity. Such calculations are predicated on the assumption that air-sea transfer dynamics are determined by bulk meteorological variables. Bulk parameterizations are desirable because if accurate, these algorithms could predict fluxes wherever the bulk atmospheric conditions are known, avoiding costly direct measurements.

Direct Covariance.

This method calculates the turbulent fluxes directly by finding the statistical cross-covariance of simultaneous measurements (vertical fluctuation w' with u', v' or T') over a finite sampling period. Fluxes are understood to occur when these turbulent fluctuations are cross-correlated. For instance, correlation between streamwise and vertical velocity fluctuations is indicative of shear stress along the mean flow. Momentum flux (Reynolds shear stress) τ is determined by

$$\vec{\tau} = -\rho\left[\langle u'w'\rangle\hat{i} + \langle v'w'\rangle\hat{j}\right]$$

or equivalently

$$\tau = -\rho\left(\langle u'w'\rangle^2 + \langle v'w'\rangle^2\right)^{1/2}$$

following the standard averaging procedure where u is the streamwise (mean) wind, v is the lateral (cross) wind, w is the vertical wind, ρ is the density of air taken from the bulk algorithm and $\langle\ \rangle$ denotes time averages. For this investigation the averages are taken over time and ergodicity is assumed, implying that the time averages will approach the ensemble averages for a large number of realizations of a particular flow. Sensible heat flux (H_s) is similarly calculated by

$$H_s = \rho c_p \langle w'T'\rangle$$

with the measured time series of absolute temperature T and the specific heat of air c_p at constant pressure.

Assuming horizontal homogeneity and stationarity such that the cross-wind contribution $\langle v'w'\rangle$ is ignored and $\tau = -\rho\langle u'w'\rangle$, the friction velocity u_* can then be obtained from

$$\tau = \rho u_*^2 \ .$$

This method also yields the cross-spectral density S_{xw} (the Fourier transform of the cross-covariance function at different time lags) defined by

$$\int_0^\infty S_{xw}(f)df = \langle x'w'\rangle = Cov(x', w')$$

where f is the frequency (Hz). S_{xw} gives contributions to the turbulent variations at different frequencies since $\langle x'w'\rangle$ is the covariance according to the general form

$$Cov(\alpha,\beta)=E[(\alpha-\mu_\alpha)(\beta-\mu_\beta)]=E(\alpha\beta)+\mu_\alpha\mu_\beta=E(\alpha\beta)\ .$$

Inertial Dissipation.

The scientific community has historically been somewhat skeptical of the inertial-dissipation method because of unresolved issues involving local anisotropy and coefficient/constant approximations [Edson et al., 1991], as well as the assumed balance between production and viscous dissipation in the turbulent kinetic energy (TKE) budget and similarity in the cascade of energy from lower frequency scales of input to higher frequency scales of dissipation [Donelan et al., 1998]. However, understanding of these problems has advanced significantly.

The inertial dissipation method is based on the Monin-Obukhov similarity theory, which postulates that the structure of turbulent flow in the surface layer is determined by the relative strength of mechanical and thermal forcing. In the inertial subrange of high frequencies utilized by this method, chosen when normalized frequency $f_n=f\,z/\overline{U}\geq 2$ [Smith and Anderson, 1984], the one-dimensional power spectral density (the Fourier transform of the autocorrelation function at different time lags) is given by

$$\int_0^\infty S_{xx}(f)df=\langle x'^2\rangle=Var(x').$$

This can be used as the Kolmogorov variance spectrum for streamwise flow assuming Taylor's hypothesis, $[k\Phi(k)=fS(f)]$ and $\left[k=2\pi f/\overline{U}\right]$, to convert wavenumber spectra to frequency spectra

$$fS_{uu}(f)=T_{uu}\alpha_u\varepsilon^{2/3}\left(\frac{2\pi f}{\overline{U}}\right)^{-2/3}$$

[Edson and Fairall, 1998]. This relation can be manipulated to yield ε, the dissipation rate of TKE. Here α_u is the one-dimensional Kolmogorov constant taken to be 0.53 [Edson and Fairall, 1998], z is the instrument height above sea level and $\overline{U}$ is the mean wind speed found by calculating the mean of the instantaneous norms of the measured wind vectors and fitting a logarithmic wind profile to obtain the 10m neutral value. Thus $\overline{U}$ represents the average speed, not the average velocity. T_{uu} is a correction for inaccuracies in using Taylor's hypotheses to estimate wavenumber spectra in the inertial subrange, given by

$$T_{uu}=1-\frac{\sigma_u^2}{9(\overline{U})^2}+\frac{2(\sigma_v^2+\sigma_w^2)}{3(\overline{U})^2}$$

[Wyngaard and Clifford, 1977] where the variances are computed from the turbulent velocities. Assuming that TKE production and dissipation are in balance implies that

$$\frac{\varepsilon \kappa z}{u_*^3} = \phi_\varepsilon(\zeta)$$

where $\zeta = z/L$ is a dimensionless height and stability parameter, L is the Monin-Obukhov length, κ is the von Karman constant taken to be 0.4 and ϕ_ε is the dimensionless dissipation function which is found from the optimized equations

$$\phi_\varepsilon(\zeta) = \frac{(1-\zeta)}{(1-7\zeta)} - \zeta, \zeta < 0$$

$$\phi_\varepsilon(\zeta) = 1 + (e-1)\zeta, \zeta > 0$$

[Edson and Fairall, 1998] and $e = 0.5\left[u'^2 + v'^2 + w'^2\right]$ is the TKE. Here L is taken to be

$$L = -\frac{u_*^3 \overline{T_v}}{g\kappa\langle w' T_v' \rangle}$$

[Donelan et al., 1997] where g is the acceleration of gravity (9.81m/s^2) and the virtual temperature T_v is related to temperature T and specific humidity m according to $T_v = T + 0.61Tm$ with the mean specific humidity taken from the bulk algorithm. These relations are then solved for the inferred momentum flux $\tau = \rho u_*^2$.

Similarly, for temperature we have $H_s = -\rho c_p u_* T_*$ and

$$\phi_{N_t}(\zeta) = \frac{N_t \kappa z}{u_* T_*^2}$$

where ϕ_{N_t} is the dimensionless dissipation function and N_t is one-half the dissipation rate of temperature variance. The former defined by Edson and Fairall [1998] as

$$\phi_{N_t}(\zeta) = (1-\zeta)^{1/6}(1-16\zeta)^{-1/2}, \zeta < 0$$

$$\phi_{N_t}(\zeta) = 1 + 6\zeta, \zeta > 0 .$$

The Kolmogorov variance spectrum for temperature is given by

$$fS_{tt}(f) = T_{tt}\alpha_t \varepsilon^{-1/3} N_t \left(\frac{2\pi f}{\overline{U}}\right)^{-2/3}$$

where α_t is the Obukhov-Corrsin constant taken to be 0.80 and the correction factor T_{tt} is given by Wyngaard and Clifford [1977] as

$$T_{tt} = 1 - \frac{\sigma_u^2}{9(\overline{U})^2} + \frac{(\sigma_v^2 + \sigma_w^2)}{3(\overline{U})^2} .$$

From these manipulations H_s is determined using ε from the velocity autocovariance spectrum.

Thus the Monin-Obukhov similarity theory hypothesizes that turbulent statistics are universal functions of the dimensionless height ζ, which is taken to be a measure of stability since ζ equals the flux Richardson number R_f which gives the ratio of buoyant production to stress production of TKE [Tennekes and Lumley, 1972].

WORK COMPLETED

The autonomous air-sea flux measurements were performed on the Buzzards Bay Tower in Massachusetts starting in December 1999. The latest data retrieved from the tower was April 2001. The boom was fabricated and deployed on the tower to test the feasibility of tower-based direct flux systems. Flow distortion studies were also performed on the meteorological measurements. The boom, sonic anemometer, and microprocessor based acquisition remain on the Buzzards Bay Tower. The NOAA National Data Buoy Center maintains wind, water vapor, air temperature, wave height, and water temperature instruments.

The instrument used was a Gill Instruments ultrasonic anemometer-thermometer that returns three orthogonal velocity components and the speed of sound sampled at a frequency of 20.83Hz. The data were automatically averaged in blocks of four data points to produce a virtual frequency of 5.21Hz. Noise in this instrument was found to be 0.05 ± 0.005m/s, producing negligible contributions to τ and H_s.

RESULTS

Speed of sound V were used to solve for the temperature time series by

$$V = 332\sqrt{\frac{T}{273.15}}$$

where T is the absolute air temperature (K) and 332 is the speed of sound at the tower for 0°C as calculated through regression of the tower temperature data.

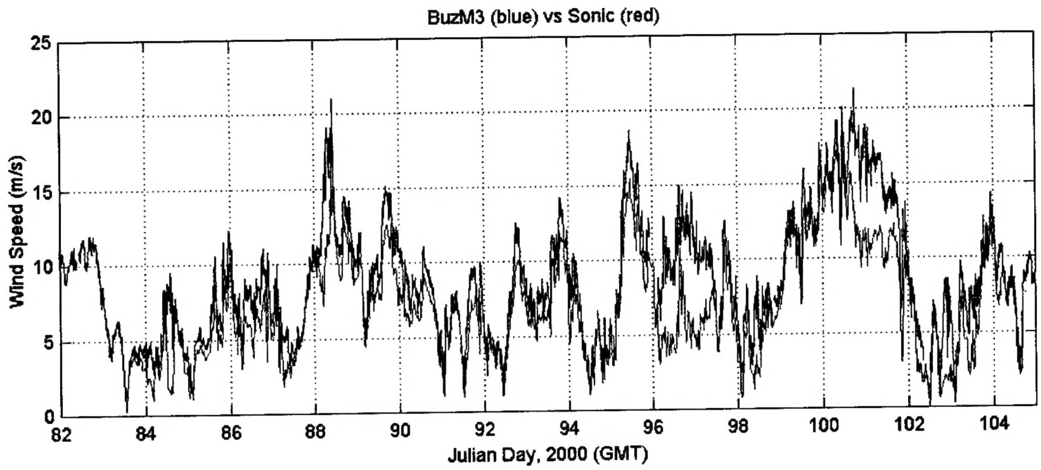

Figure 1: Comparison of a 24-day time series of wind speed measurements on the Buzzards Bay Tower. The WHOI sonic anemometer (red) is compared with the NOAA NDBC Young propeller-vane anemometer (blue). The sonic anemometer is positioned 4m on a boom extension and the propeller-vane is positioned directly on top of the tower on an instrument frame.

The instrument is deployed horizontally on the upper platform of the USCG BUZM3 tower in Buzzards Bay, Massachusetts, located at (41.40°N, 71.03°W). Approximate dimensions for the tower superstructure are 21m height and 7m width and depth. Water depth at this location is approximately 20m, and the tower is 6.6km from the nearest shore (Cuttyhunk Island). The instrument height was 15.6m, oriented to face the summer modal wind direction (215° from north) with the axis of the instrument at 284° (WNW). This direction provides wind and waves with essentially unlimited fetch. Wind speed at the tower generally has values of 0-15m/s. The ultrasonic anemometer was horizontally extended 4m from the edge of the tower, mounted on a metal boom. The USCG platform was generally unmanned except when data was retrieved.

Figure 1 shows a comparison between the WHOI boom-mounted sonic anemometer and the NOAA NDBC propeller-vane anemometer. While there is good alignment in the structure of the wind field, some discrepancies are evident. This is due to sheltering and flow distortion of the tower on the boom, which is dependent on the wind direction. Figure 2 shows that when winds are not aligned north and south, there are flow distortion effects in the mean wind speed.

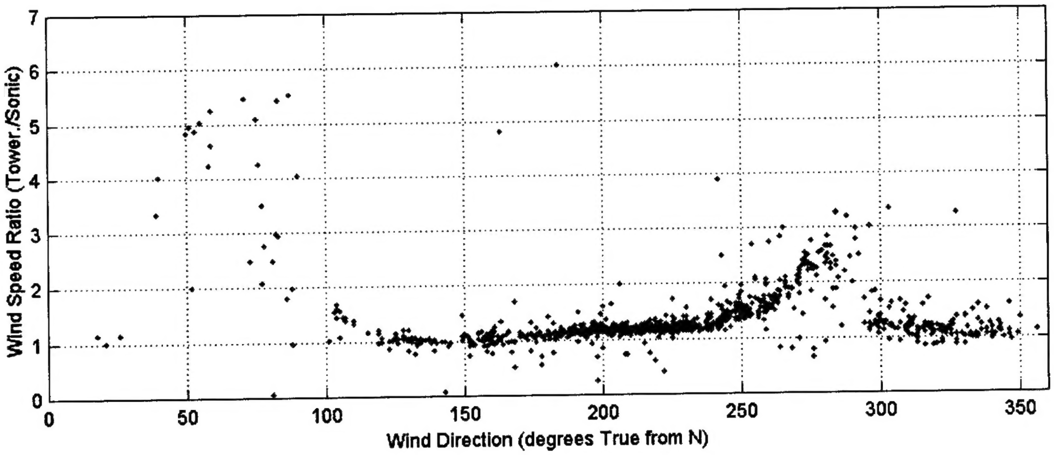

Figure 2: Ratio of propeller-vane anemometer to sonic anemometer measurements. Winds from behind the tower structure are strongly distorted.

Initial estimates of tower flow distortion were generated from a simple potential flow algorithm where the tower platform was assumed to be a (point dipole) cylinder of radius R and strength $\mu = R^2 2\pi U_f$ in freestream velocity U_f. This analysis indicated that distortion at the 4-m extension in the plane of the platform would be roughly 6% depending on orientation. Analysis at the tower indicates that the true distortion may be twice this value.

An obstruction in a turbulent flow field produces a turbulent wake that is different from the unobstructed flow that is supposed to be measured. Data from the tower were analyzed to approximate this flow distortion by the ratio $d = \left|\langle v'w'\rangle / \langle u'w'\rangle\right|$, which by the assumptions of horizontal homogeneity, stationarity, and constant stress should have the property d << 1 in the absence of flow disturbance (net stress is expected to be aligned with mean wind). This ratio was found to be 0.10 for all composite fluxes, which justifies the simplifying assumption of $\tau = -\rho\langle u'w'\rangle$ since neglecting the cross-stream contribution changes τ by a factor of $\sqrt{1^2 + 0.10^2} \cong 1.005$ or less than 1%. Some of the cross-wind stress values were made smaller by significant cancellation associated with sign reversal of the meandering cross-wind. Smith [1980] rejected data for which d > 0.5, fearing contamination by platform motion. Edson et al. [1991] used data for which d=0.08 but considered d = 0.57 unacceptably large.

The anemometer coordinate system was rotated about the x-axis [$X_f = X_o$, $Y_f = -Z_o$, $Z_f = Y_o$] to make the z-axis vertical. Wind velocity components were aligned along the mean wind direction for each sample such that the mean vertical and lateral wind components were zero. This standard procedure corrected for an average vertical tilt of 6.5° ± 0.2°, which by the assumption of incident horizontal wind implies that the anemometer was tilted 6.5° to the horizontal plane. Small scatter in this value indicates that the horizontal

assumption was valid. Accurate tilt correction is crucial since small deflections of order 1° can produce large errors in the calculated stress [Donelan, 1990; Mahrt et al., 1996].

The speed of sound data was also converted to a temperature time series. All time series were then linearly detrended to produce the turbulent fluctuations u', v' and w' and temperature variation T' to be used in flux calculations. Data from the anemometer was temporally correlated with bulk atmospheric data at the tower taken from the National Data Buoy Center (NDBC) web archive (http://www.ndbc.noaa.gov/station_page.phtml?$station=buzm3).

Spectra were averaged over time periods with similar atmospheric conditions, particularly wind speed and dimensionless dissipation function ϕ_ε, generating composite spectra which possessed greater statistical significance since sampling variability was reduced. These common characteristics define the data as part of an ensemble, and data from periods of rapid atmospheric changes were rejected since fluxes can change quite dramatically over time [Fairall and Larsen, 1986; Large and Pond, 1981]. These composite spectra were then smoothed using a median filter. For each power spectrum a Hamming tapering window was used to reduce overestimation of spectral energy in the inertial subrange due to finite sampling [Kaimal and Kristensen, 1991].

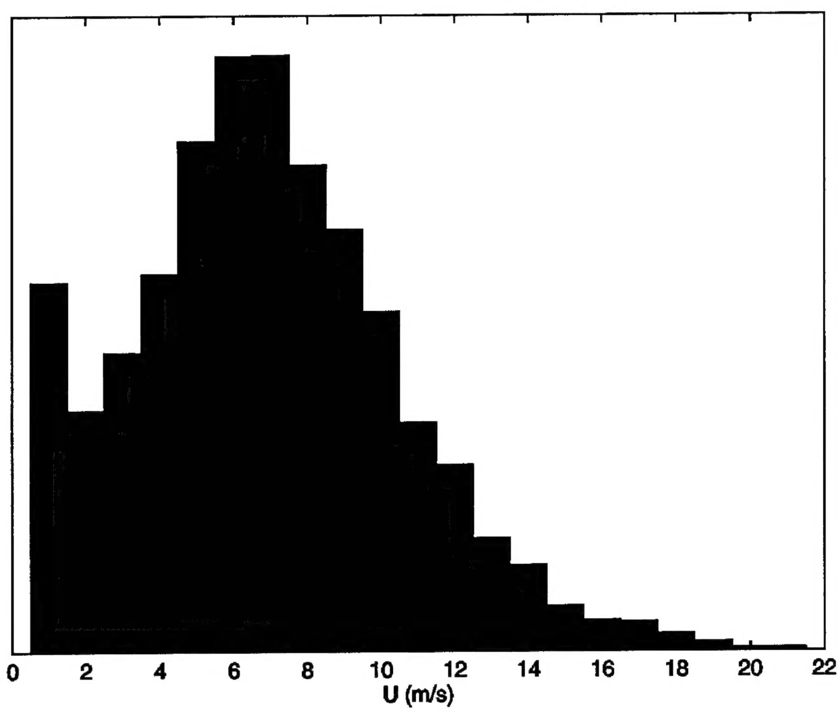

Figure 3: Histograms of sonic anemometer winds during measurements December 1999 to April 2001.

Figure 3 shows the histograms of winds measured with the sonic anemometer from December 1999 to April 2001. Representative data from consecutive files, during which atmospheric conditions were virtually constant, are presented in Table 1.

Table 1. Atmospheric conditions during data acquisition.

Start Time (UTC)	Run	Date (1999)	Files	$\overline{U}$ (m/s)	T_{air} (°C)	T_{sea} (°C)	P_{atm} (mb)	RH (%)
1729	1	24 July	5	6.96	22.7	20.5	1008.6	94

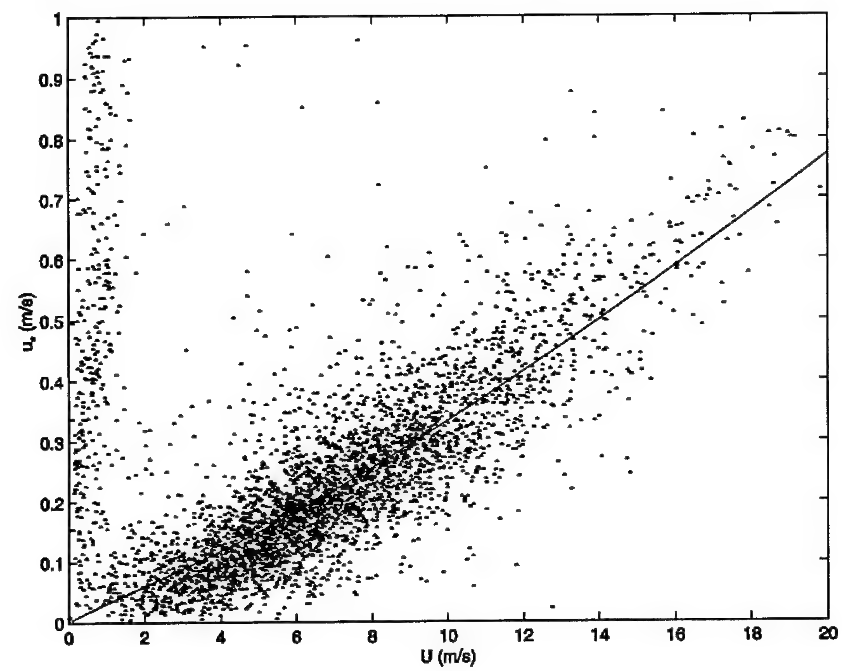

Figure 4: Friction velocity versus 10-m wind speed. Also shown for comparison is the bulk model from Fairall et al., 1996.

Any results for $\overline{U}$ < 3m/s should be viewed with some suspicion due to the dependence of wind stress on the method of computation [Mahrt et al., 1996]. In Table 2, calculations of direct covariance fluxes are compared to results from the bulk algorithm. Values were computed from detrended time series, not by integration of spectral estimates.

Table 2. Comparison between direct covariance and bulk algorithm.

Run	$-\rho\langle u'w'\rangle$	Bulk τ (N/m²)	$\rho c_p\langle w'T'\rangle$	Bulk H_s (W/m²)	L (m)	z/L	Class
1	0.0625	0.0451	-14.4	-16.4	76.3m	0.20	Stable

Here the general classification $L > 0$ for stable/stratified conditions and $L < 0$ for unstable/convective conditions has been used, where L is calculated from the direct covariance friction velocity.

Good agreement is found with the sensible heat flux regression of Smith [1980], which had a correlation coefficient of 0.98 for the Stanton number (heat flux coefficient). Comparisons are made in Table 3.

Table 3. Comparison among sensible heat values.

Run	$\rho c_p \langle w'T' \rangle$	**Inertial Dissipation**	**Bulk**	**Smith [1980]**
1	-14.4	-13.0	-16.4	-15.1

Values of the friction velocity u_* (m/s) from this experiment are presented in Table 4 for easy comparison.

Table 4. Comparison among friction velocity values and scatter (standard deviation).

Run	**Direct covariance**	**Standard Deviation**	**Inertial dissipation**	**Standard Deviation**	**Bulk Algorithm**
1	0.230	0.005	0.259	0.013	0.196

There is reasonable agreement among the friction velocity values, and it has been postulated that the direct covariance and inertial dissipation values may differ due to the presence of swell [Donelan, 1997] or unusually large stability/instability [Large and Pond, 1981]. Also, it has been established [Edson et al., 1991] that the inertial-dissipation method is much less affected by platform flow distortion relative to the direct covariance method, which may account for some of the discrepancies.

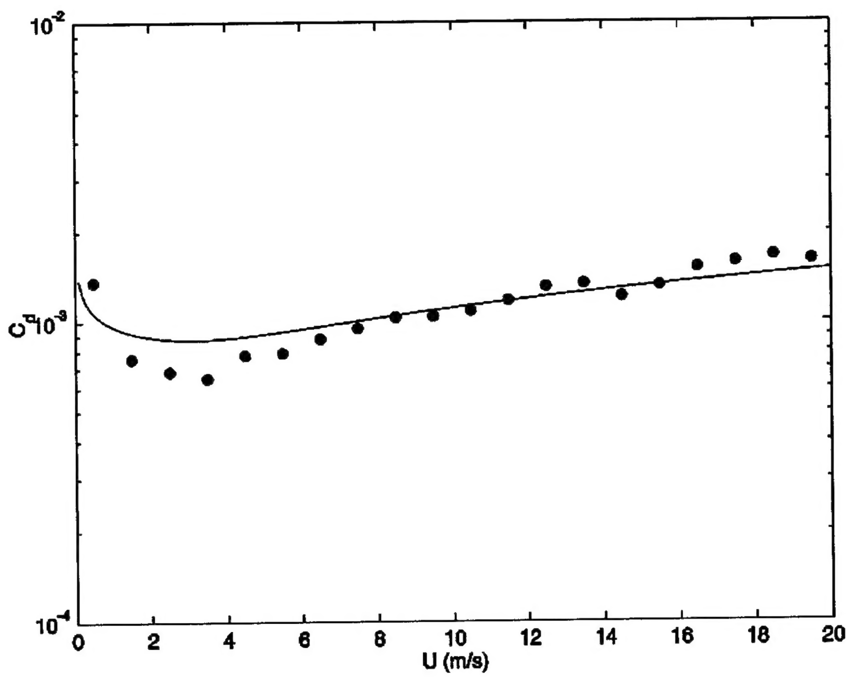

Figure 5: Drag coefficient compared with bulk parameterization model versus 10-m wind speed for the Buzzards Bay Tower.

Variation of the individual u_* measurements follows the expected linear relationship to wind velocity, where larger fluxes are associated with faster wind speeds (Figure 4). Ensemble-averaged drag coefficients are shown in Figure 5. Energy (and momentum) are transferred from the mean flow to large-scale turbulent eddies, followed by energy exchange to progressively smaller eddies through an energy cascade driven by vortex

stretching [Tennekes and Lumley, 1972], and eventually the energy is converted to heat through small-scale (Kolmogorov microscale) viscous dissipation. Therefore large-scale turbulent eddies transport momentum within the atmospheric boundary layer. The frequency f_m at the spectral peak gives the dominant eddy time scale $\tau_m = 1/f_m$ to be $\tau_m \approx$ 10.8s for stable conditions, yielding a characteristic time scale for the motion of these large turbulent eddies in the boundary layer since each eddy size is associated with a particular time scale. The value at the spectral peak ($f_n = 0.2$) agrees reasonably well with that of Smith and Anderson [1984], who obtained $f_n = 0.3$ for stable wind stress cospectrum. It should be noted that Large and Pond [1981] found significant stability dependence of the spectral peaks.

It has been noted [Edson et al., 1991; Geernaert et al., 1988; Large and Pond, 1981] that the inertial-dissipation technique gives the most accurate results in near-neutral conditions $(-0.45 \leq z/L \leq 0.15)$. For this reason, the presence of very stable atmospheric conditions $(z/L \geq 0.15)$ during data collection suggests that more emphasis be placed on the direct covariance measurements.

One of the assertions of Monin-Obukhov similarity theory is that $S_{vv}(f) = S_{ww}(f) = (4/3)S_{uu}(f)$ at neutral stability for frequencies in the inertial subrange assuming local isotropy (turbulent statistics invariant under rotation of coordinates). Values were found to be $S_{vv}(f)/S_{uu}(f) = 1.27$ and $S_{ww}(f)/S_{uu}(f) = 1.47$.

Good agreement is found between the turbulence level $\sigma_u/U_p = 0.075$ and the values 0.080 from the regression line of Smith [1980] and 0.086 from the regression line of Large and Pond [1981], where U_p is the wind speed at the platform and σ_u is the standard deviation of the streamwise fluctuations. This indicates that the variability is roughly correct, which seems to contradict the 2% correction produced by T_{uu} for Edson and Fairall [1998] since this study found corrections smaller by an order of magnitude.

The $f^{-2/3}$ power law for the inertial subrange is clearly seen on all spectra for mean wind and virtual temperature autocorrelations, indicating that the flows were sufficiently turbulent to warrant application of the Kolmogorov variance spectrum.

IMPACT/APPLICATIONS

Investigating direct fluxes under high wind conditions is difficult due to the adverse conditions and low frequency of high wind episodes in most climates. Autonomous, tower-based time series of direct fluxes is one possible strategy to overcome this difficulty. Capturing high wind states is possible with continuous measurements. This project helped demonstrate that tower based fluxes could (1) provide continuous measurements for long duration of air-sea exchange variability that could be used in mesoscale climate predictions; and (2) could help determine the long term feasibility of an autonomous direct flux system that can be deployed in locations that encounter greater wind speeds.

Analysis of the autonomous flux measurements indicates that utilization of the Buzzards Bay tower for the measurement of turbulent fluxes is feasible. Reasonable agreement among different methods of calculation implies that the theoretical formulations and algorithm implementations are correct. In addition, good agreement with published results is encouraging. These include:

- spectral peaks
- local isotropy
- turbulence level
- variation of u_* with wind speed

Small scatter in the tilt angle (0.2°) supports the important assumption of steady horizontal flow. Flow distortion is thought to be acceptable at 4-m extension. Placement of an autonomous system on the tower should be closer to the mean sea surface to insure measurements are in the boundary layer.

Maintaining a direct flux system at the Buzzards Bay Tower should be considered and would include the following:

- Telemetered acquisition and solar power.
- Automatic analysis of data.
- Thorough analysis of flow distortion by comparison tests at different locations on the platform.
- Addition of sensors to establish time series for fast response water vapor, mean wave direction, and current velocity.
- Acquisition of data for solar and IR radiation at/near the tower.

RELATED PROJECTS

The system on the Buzzards Bay Tower could provide data in support of the ONR CBLAST-Low Study. The Buzzards Bay Tower is less than 30 km from the future CBLAST tower site and could prove to be a useful complement for tower based fluxes, mesoscale features, and mean meteorological variables.

Acknowledgments. Many individuals at WHOI shared in the responsibility and success of this project including, Jesse Chuhta, Jonathan Ware, Sean McKenna, Jay Sisson, Steve Faluotico, and Jim Edson.

REFERENCES

M.A. Donelan, 1990: Air-sea interaction. *The Sea,* B. LeMehaute and D. Hanes, Eds., Vol. 9A, Wiley, 239-292.

---------- et al., 1997: The Air-Sea Momentum Flux in Conditions of Wind Sea and Swell. *J. Phys. Oceanogr.,* **27**, 2087-2099.

J.B. Edson et al., 1991: A Study of the Inertial-Dissipation Method for Computing Air-Sea Fluxes. *J. Geophys. Res.*, **96**, 10,689-10,711.

---------- and C.W. Fairall, 1998: Similarity Relationships in the Marine Atmospheric Surface Layer for Terms in the TKE and Scalar Variance Budgets. *J. Atmos. Sci.*, **55**, 2311-2328.

C.W. Fairall and S.E. Larsen, 1986: Inertial-Dissipation Methods and Turbulent Fluxes at the Air-Ocean Interface. *Boundary-Layer Meteorol.*, **34**, 287-301.

---------- et al., 1996: Bulk parameterization of air-sea fluxes for Tropical Ocean-Global Atmosphere Coupled-Ocean Atmosphere Response Experiment. *J. Geophys. Res.*, **101**, 3747-3764.

G.L. Geernaert, 1988: Measurements of the angle between the wind vector and wind stress vector in the surface layer over the North Sea. *J. Geophys. Res.*, **93**, 8215-8220.

J.C. Kaimal and L. Kristensen, 1991: Time Series Tapering for Short Data Samples. *Boundary-Layer Meteorol.*, **57**, 187-194.

W.G. Large and S. Pond, 1981: Open Ocean Momentum Flux Measurements in Moderate to Strong Winds. *J. Phys. Oceanogr.*, **11**, 324-336.

W.T. Liu et al., 1979: Bulk Parameterization of Air-Sea Exchanges of Heat and Water Vapor Including the Molecular Constraints at the Interface. *J. Atmos. Sci.*, **36**, 1722-1735.

L. Mahrt et al., 1996: Sea surface drag coefficients in the Riso Air Sea Experiment. *J. Geophys. Res.*, **101**, 14,327-14,335.

E. Mollo-Christensen, 1979: Upwind Distortion Due to Probe Support in Boundary-Layer Observation. *J. Appl. Meteor.*, **18**, 367-370.

S.D. Smith, 1980: Wind Stress and Heat Flux over the Ocean in Gale Force Winds. *J. Phys. Oceanogr.*, **10**, 709-726.

----------, 1988: Coefficients for Sea Surface Wind Stress, Heat Flux, and Wind Profiles as a Function of Wind Speed and Temperature. *J. Geophys. Res.*, **93**, 15,467-15,472.

---------- and R.J. Anderson, 1984: Spectra of Humidity, Temperature, and Wind Over the Sea at Sable Island, Nova Scotia. *J. Geophys. Res.*, **89**, 2029-2040.

H. Tennekes and J.L. Lumley, 1972: *A First Course in Turbulence.* The MIT Press.

J.C. Wyngaard and S.F. Clifford, 1977: Taylor's hypothesis and high frequency turbulence spectra. *J. Atmos. Sci.*, **34**, 922-929.